Can. J. Remote Sensing, Vol. 34, No. 3, pp. 245–258, 2008

Sensitivity of a carbon and productivity model to climatic, water, terrain, and biophysical parameters in a Rocky Mountain watershed

Shiyong Xu, Derek R. Peddle, Craig A. Coburn, and Stefan Kienzle

Abstract. Net primary productivity (NPP) is a key component of the terrestrial carbon cycle and is important in ecological, watershed, and forest management studies, and more broadly in global climate change research. Determining the relative importance and magnitude of uncertainty of NPP model inputs is important for proper carbon reporting over larger areas and time periods. This paper presents a systematic evaluation of the boreal ecosystem productivity simulator (BEPS) model in mountainous terrain using an established montane forest test site in Kananaskis, Alberta, in the Canadian Rocky Mountains. Model runs were based on forest (land cover, leaf area index (LAI), biomass) and climate–water inputs (solar radiation, temperature, precipitation, humidity, soil water holding capacity) derived from digital elevation model (DEM) derivatives, climate data, geographical information system (GIS) functions, and topographically corrected satellite imagery. Four sensitivity analyses were conducted as a controlled series of experiments involving (*i*) NPP individual parameter sensitivity for a full growing season, (*ii*) NPP independent variation tests (parameter $\mu \pm 1\sigma$), (*iii*) factorial analyses to assess more complex multiple-factor interactions, and (*iv*) topographic correction. The results, validated against field measurements, showed that modeled NPP was sensitive to most inputs measured in the study area, with LAI and forest type the most important forest input, and solar radiation the most important climate input. Soil available water holding capacity expressed as a function of wetness index was only significant in conjunction with precipitation when both parameters represented a moisture-deficit situation. NPP uncertainty resulting from topographic influence was equivalent to 140 kg C ha^{-1}·$year^{-1}$. This suggested that topographic correction of model inputs is important for accurate NPP estimation. The BEPS model, designed originally for flat boreal forests, was shown to be applicable in mountainous terrain given appropriate image terrain corrections using the SCS+C approach. Rocky Mountain carbon dynamics were simulated with average annual NPP of Kananaskis forests estimated at 4.01 t C ha^{-1}·$year^{-1}$ and compared favourably with the field plot estimate of 4.24 t C ha^{-1}·$year^{-1}$ for this area.

Résumé. La productivité primaire nette (PPN) constitue un élément clé du cycle du carbone terrestre et elle est importante pour les études écologiques, les études de bassins versants et de gestion forestière et, plus généralement, pour la recherche sur les changements climatiques à l'échelle du globe. La détermination de l'importance relative et de l'amplitude de l'incertitude des intrants aux modèles de PPN est essentielle pour la production de rapports adéquats sur le carbone au-dessus de zones plus vastes et pour des périodes plus longues. Dans cet article, on présente une évaluation systématique du modèle BEPS (« boreal ecosystem productivity simulator ») en terrain montagneux en utilisant un site de forêt montagnarde bien connu situé à Kananaskis, en Alberta, dans les montagnes Rocheuses canadiennes. Les intrants de base utilisés pour faire tourner le modèle étaient reliés à la forêt (couvert, LAI, biomasse) et au climat et à l'eau (rayonnement solaire, température, précipitation, humidité, capacité de rétention de l'eau du sol) dérivés des dérivées d'un modèle numérique d'altitude (MNA), des données climatiques, des fonctions SIG et d'images satellitaires corrigées pour les effets topographiques. Quatre analyses de sensibilité ont été réalisées sous forme d'une série contrôlée d'expériences comprenant (*i*) la sensibilité des paramètres individuels de PPN au cours d'une saison de croissance entière, (*ii*) tests de variation indépendante de PPN (paramètre $\mu \pm 1\sigma$), (*iii*) analyses factorielles pour évaluer les interactions multifacteurs plus complexes, et (*iv*) correction topographique. Les résultats, validés par rapport à des mesures sur le terrain, ont montré que la PPN modélisée était sensible à la plupart des intrants mesurés dans la zone d'étude, le LAI et le type de forêt étant les intrants les plus importants, et le rayonnement solaire étant l'intrant climatique le plus important. La capacité de rétention de l'eau disponible dans le sol en tant que fonction de l'indice d'humidité était significative seulement en conjonction avec les précipitations lorsque les deux paramètres présentaient une situation de déficit d'humidité. L'incertitude de PPN résultant de l'influence topographique était équivalente à 140 kg C ha^{-1}·an^{-1}. Ceci laissait supposer que la correction topographique des intrants du modèle était importante pour l'estimation précise de PPN. Le modèle BEPS, conçu au départ pour les forêts boréales à relief plat, s'est avéré applicable dans les régions montagneuses après application des corrections appropriées de terrain aux images en utilisant l'approche SCS+C. La dynamique du carbone des montagnes Rocheuses a été simulée avec des valeurs annuelles moyennes de PPN pour les forêts de Kananaskis estimées à 4,01 t C ha^{-1}·an^{-1} et celle-ci se comparait avantageusement à la valeur de 4,24 t C ha^{-1}·an^{-1} observée sur la parcelle expérimentale pour cette zone.
[Traduit par la Rédaction]

Received 23 January 2008. Accepted 20 May 2008. Published on the *Canadian Journal of Remote Sensing* Web site at http://pubs.nrc-cnrc.gc.ca/cjrs on 29 August 2008.

S. Xu, D.R. Peddle,[1] C.A. Coburn, and S. Kienzle. Department of Geography, University of Lethbridge, Lethbridge, AB T1K 3M4, Canada.

[1]Corresponding author (e-mail: derek.peddle@uleth.ca).

Introduction

The balance of atmospheric CO_2 exchanges with oceans and terrestrial ecosystems has been disturbed by human activities over the last 100–200 years, and it is widely believed that higher atmospheric concentrations of greenhouse gases are contributing to global warming (Houghton and Hackler, 1995; Cao and Woodward, 1998; Falkowski et al., 2000). Forests are estimated to account for more than 75% of the carbon (C) stored in global terrestrial ecosystems and approximately 40% of the annual carbon exchange between the atmosphere and the terrestrial biosphere (Hamilton et al., 2002). Canada has about 10% of the world's forests, and this coupled with the greater sensitivity of northern regions to climate change means that Canadian forests have an important role in the global carbon cycle. Because of the spatial extent of forest biomes, the relationships of forest biomes to climate, and the importance of forest biomes as a carbon stock, it is necessary to understand the function of ecosystem processes. The processes driving ecosystem carbon fluxes include photosynthesis, plant respiration, and soil respiration. Net primary productivity (NPP) is defined as the difference between plant photosynthesis and respiration, and the difference between NPP and soil respiration is defined as net ecosystem productivity (NEP) (Cao and Woodward, 1998). NPP is a key factor for quantifying forest growth, in terrestrial carbon cycling, and in studies of global climate change. However, it is difficult to extrapolate carbon dynamics from regional to global scales. For example, Canadian forests may be either a net source of carbon (Kurz and Apps, 1999) or a carbon sink (Chen et al. 2000). According to Houghton (2002), the difference between the net terrestrial sink and emissions from land-use change, shown as a residual terrestrial sink, is also not well understood globally. Therefore, further research is required to better understand the terrestrial ecosystem carbon cycle.

The influence of environmental variability on forest carbon balances can be studied directly with field measurements of site-specific carbon fluxes. However, this is impractical over large areas and as a means of capturing sufficiently the spatial variability. Further, due to terrestrial heterogeneity and distribution, spatial and temporal gaps in measurement records are inevitable. Moreover, it is difficult to execute plot-level experimental studies for larger environmental changes (Amthor et al., 2001). It is therefore necessary to use computer models in conjunction with field measurements to provide the spatial and temporal coverage required for broad, comprehensive studies. Models can also be used to help understand global carbon cycling (Liu et al., 2002) and to conduct retrospective analyses of ecosystem responses to past climatic variability (Cao and Woodward, 1998). Various models have been applied to make spatially comprehensive estimates of carbon for large regions in the world. At the same time, ecological models have been built at a variety of spatial and temporal scales and locations and with different driving inputs and assumptions.

Accordingly, model accuracy must be evaluated before ecosystem models can be applied to a specific location or biome with confidence over larger areas and longer time scales. This can be done by comparing model predictions with independent field measurements. For example, the boreal ecosystem productivity simulator (BEPS) is a remote sensing approach to quantifying the terrestrial carbon cycle (Liu et al., 2003) that has been used for mapping NPP in Canada (Liu et al. 1997; 2002). In this paper, the focus is on the use and analysis of BEPS in complex mountainous terrain in the Canadian Rockies. To assess model applicability in this montane environment, it was necessary to first run the model varying input parameters and then assess the effect on model output resulting from controlled parameter changes. This work also tests the robustness of BEPS, given that this model was designed for flat, boreal forests but in this paper is being tested in mountainous terrain for the first time. The test is reasonable, given the broad similarity of the major boreal and montane forest species involved (e.g., spruce, pine, aspen) and the existence of appropriate parameter constants (if needed) from related models, e.g., FOREST-BGC (Running and Coughlan, 1988); indeed, the larger issue in terms of remote sensing image spectral response may well be the differences in terrain geometry, which we address in this study using advanced topographic correction.

The sensitivity analyses were designed to test model performance for the variety and range of input parameters in the study area. Four main objectives were identified to achieve this: (*i*) quantify the sensitivity of BEPS to its main input variables, with validation against field-determined NPP; (*ii*) determine the most critical inputs to the BEPS model; (*iii*) assess the sensitivity of BEPS to the topographic influence in this mountainous area, and therefore the robustness of the model for this purpose; and (*iv*) estimate NPP carbon dynamics in the study area using topographically corrected data inputs.

Process-based ecosystem models and BEPS

Computer simulation modeling of the terrestrial carbon cycle is a major focus in global change research. Process-based models are based on current understanding of ecosystems and the mechanisms of biomass production, plant–environmental interaction, and an ability to model vegetation growth by simulating the processes of carbon assimilation, autotrophic and heterotrophic respiration, and decomposition based on inputs of climate drivers and site parameters (Friend et al., 1997).

BEPS (Liu et al., 1997) is a daily time step model derived from the FOREST-BGC family of models (Running and Coughlan, 1988) for application at the forest-stand to regional scales. The biophysical principles in FOREST-BGC were adopted for BEPS model development because FOREST-BGC has been well documented and tested with measured NPP over various climatic zones (Running, 1994). BEPS also draws on BIOME-BGC; however, it accounts for the effects of canopy architecture on radiation interception (Chen et al., 1999). BEPS provides an advanced treatment of radiation transport through the canopy, including separation of sunlit and shaded leaf area.

Leaf-level photosynthesis is related to remotely sensed leaf area index (LAI) estimates. The treatment of highly clumped canopies is a special feature for boreal conifer forests. Important inputs for BEPS are land cover, leaf area index (LAI), biomass (Bio), soil available water-holding capacity (AWC), and a series of daily meteorological variables (shortwave radiation, minimum and maximum temperature, humidity, and precipitation). As output, BEPS predicts photosynthesis, plant growth and maintenance respiration, litter production, decomposition, transpiration and precipitation interception losses, soil water evaporation, and soil water status.

Methods

Study area

The study area located in the Kananaskis region of Alberta in the Canadian Rocky Mountains was centred at 51°1′13″N, 115°4′20″W and encompassed 38.7 km^2 of the watershed that drains into Barrier Lake in the northern portion of Kananaskis Country and its network of provincial parks. The area has an elevation range from 1316 to 2186 m and is situated in a broader ecological zone characterized by varying soils and forests due to its climatic diversities and complex terrain. The dominant conifer trees in the area include lodgepole pine (*Pinus contorta* var. *latifolia* Dougl. ex. Loud), white spruce (*Picea glauca* (Moench) Voss), and Douglas fir (*Pseudotsuga menziesii* (Mirb.) Franco). The dominant deciduous tree species are trembling aspen (*Populus tremloides* Michx.) and balsam poplar (*Populus balsamifera* L.). Field measurements were obtained from stands of lodgepole pine, white spruce, trembling aspen, white spruce, and mixed forest. The mixed forest stands were identified as having secondary tree species that made up greater than 20% of the overstory canopy (Archibald et al., 1996). This modeling experiment was conducted from June to August in 2003.

Field, image, terrain, and climate data collection and preprocessing

Forest plot measurements

Field data were obtained at 76 plots covering homogeneous areas of forest terrain. The plot size was either 10 m × 10 m or 20 m × 20 m, as dictated by local variability in this complex environment. Standard measurements recorded at each plot included diameter at breast height (DBH), tree height, height to canopy, crown diameter, geographical coordinates, slope, and aspect. LAI data were obtained using TRAC, LAI-2000, and hemispherical photography (Hall et al., 2003). Five differentially corrected global positioning system (GPS) points, one at plot centre and one at each corner, were recorded for each plot.

Field end-member spectra collection

An Analytical Spectral Devices (ASD) full-range (350–2500 nm) spectroradiometer was used to measure the spectral signatures of dominant forest species sampled from the study area. Using the field methods described by Peddle (1998), end-member component spectra for sunlit background, sunlit canopy, and shadow were collected using direct measurements, optically thick stacks, and shadowed targets, respectively. All ASD radiance measurements were then corrected to reflectance using measured coincident irradiance from a calibrated Spectralon® white reference panel. The reflectance data of end-members were used for the estimation of leaf area index and biomass.

Satellite imagery and preprocessing

Digital multispectral IKONOS satellite data were acquired on 27 August 2001 at a solar zenith angle of 42.57° and solar azimuth angle of 157.21° with a nominal spatial resolution of 4 m. This was the closest available acquisition date that was appropriate for use with the 2003 field season. For this study, multispectral bands 2 (green), 3 (red), and 4 (near infrared, NIR) were chosen, with band 1 excluded due to atmospheric scattering in this blue band.

Image preprocessing was conducted for the purpose of deriving land cover type and leaf area index. This involved radiometric, atmospheric, geometric, and topographic correction. Radiometric image calibration used post-launch IKONOS calibration coefficients to convert digital numbers (DN) to top-of-the-atmosphere (TOA) radiance. A simple dark object subtraction technique was used for atmospheric correction to convert TOA radiance to surface reflectance. Geometric correction of the imagery used GPS points for transformation and registration to Universal Transverse Mercator (UTM) coordinates for use with GPS plot locations at subpixel scale. Topographic correction was achieved using the SCS+C method (Soenen et al., 2005), which is based on sun–canopy–sensor (SCS) geometry (Gu and Gillespie, 1998) and a C-correction formulation (Teillet et al., 1982). The SCS framework is more appropriate than the sun–terrain–sensor (STS) geometry that has characterized most conventional topographic correction methods. SCS+C is an improvement on SCS that was shown both theoretically and empirically by Soenen et al. (2005) as the best correction based on extensive testing and comparisons in this Kananaskis study area. We note that, as with any study, any errors in these various preprocessing steps can affect modeled output and validation results; however, in this study these are not expected to change the main interpretations and conclusions.

Climate and digital elevation data

To parameterize the BEPS model, climate data for the summer of 2003 were obtained from the Kananaskis climate station, located at 51°2′N, 115°2′W and situated 2.2 km from the centre of the study site. Data were logged at hourly intervals and converted into daily average data. These included solar radiation (kJ·m^{-2}·day^{-1}), minimum temperature (°C), maximum temperature (°C), precipitation (mm), and relative humidity (%).

A digital elevation model (DEM) with a 25 m pixel size was obtained from the Miistakis Institute of the Rockies, which performed local adjustments to a provincial government DEM

Table 1. BEPS model inputs held constant in the analysis.

BEPS parameter	Conifer	Deciduous	Mixed
Max. stomatal conductance ($mm \cdot s^{-1}$)	1.6	2.5	2.0
Max. photosynthetic rate ($\mu mol \cdot m^{-2} \cdot s^{-1}$)	5.0	5.0	5.0
Leaf maintenance respiration ($g \cdot kg^{-1} \cdot day^{-1}$)	0.2	0.4	0.3
Stem maintenance respiration ($g \cdot kg^{-1} \cdot day^{-1}$)	0.2	0.2	0.2
Root maintenance respiration ($g \cdot kg^{-1} \cdot day^{-1}$)	0.4	1.1	0.7

Note: Values in the table correspond to the default FOREST-BGC parameters for the Rocky Mountains.

dataset. Using field control points, the DEM and satellite image data were coregistered, with the nearest neighbour DEM pixel used with each image pixel. Terrain slope and aspect were derived from the DEM for use with the climate data analysis. We note that, as studied in Band (1993), the impact of spatial resolution and aggregation can affect terrain analysis and processing; however, any systematic study of those potential affects was well outside the scope of this study.

BEPS model parameterization

A subset of the BEPS model inputs was selected for analysis based on factors such as importance in the model derivation, availability of data, and the existence of reasonable values to use as constants for those variables not included in the sensitivity study. The forest biophysical and climate–water inputs could be derived from available field, remote sensing, and terrain data and were deemed important for study with BEPS. The remaining inputs dealt with plant physiology for which neither field nor remote sensing – GIS data existed. These inputs were instead parameterized using appropriate constants (**Table 1**) from the literature based on default values for Rocky Mountain ecosystems from the FOREST-BGC model (Running et al., 1987; Running and Coughlan, 1988), the model upon which BEPS is based. Derivation of the forest biophysical and climate–water inputs that were analyzed in this paper are shown in **Tables 3** and **4** and described in the following subsections.

Forest classification

A supervised maximum likelihood (ML) algorithm was used to classify forest land cover at the study site. The classification was based on the IKONOS green, red, and NIR bands that were topographically corrected using SCS+C. The forest land cover classes for conifer, deciduous, and mixed forest were derived corresponding to suitable regional inputs to BEPS of interest in this research. Individual class accuracy was estimated based on the 76 field plots and ranged from 84% for conifer to 60% for mixed forests, the latter being more complex and a class not emphasized in the field data collection in terms of representation. The resulting land cover map from classification of the SCS+C topographically corrected imagery is shown in **Figure 1**.

LAI and biomass estimation using spectral mixture analysis

Spectral mixture analysis (SMA) was used to estimate LAI and biomass, based on earlier work in Kananaskis and elsewhere that showed SMA is well suited for providing accurate biophysical–structural information, and with consistent and considerable improvements over vegetation indices (Hall et al., 1995; 2003; Peddle et al., 1999; 2001; Peddle and Johnson, 2000). SMA was used to derive the subpixel-scale fractions of sunlit canopy, sunlit background, and shadow, with the latter used as the biophysical predictor. The process for estimating LAI and aboveground biomass involved deriving field estimates at each plot, relating those to the SMA shadow (*S*) fraction, and applying that throughout the full image using the following three steps.

Table 2. Empirical equations for estimating biomass by tree species.

Trembling aspen	$0.34961 + 0.01916(DBH)^2H$
Lodgepole pine	$8.24948 + 0.01597(DBH)^2H$
White spruce	$6.09159 + 0.14990(DBH)^2H$
Poplar	$10.81060 + 0.01352(DBH)^2H$

Note: DBH, tree diameter at breast height; *H*, tree height.

Table 3. BEPS inputs tested and their measured values in the study area.

Variable	Mean	Max.	Min.
LAI (conifer)	3.2	8.0	0.5
Rad ($kJ \cdot m^{-2} \cdot day^{-1}$)	20 960	70 000	0
T_{max} (°C)	23.7	33.0	11.0
T_{min} (°C)	5.5	15.7	–3.1
PPT ($mm \cdot day^{-1}$)	1.5	24.9	0
Hm ($g \cdot kg^{-1}$)	6.8	11.7	2.6
Bio ($t \cdot ha^{-1}$)	141	250	52
AWC (m)	0.15	0.25	0.05

Table 4. Ranges of inputs and steps for BEPS model runs.

Variable	Max.	Min.	Steps
LAI (conifer)	16.0	1.0	1
Rad ($MJ \cdot m^{-2} \cdot day^{-1}$)	70	0	3, 11
T_{max} (°C)	33	11	2
T_{min} (°C)	16	–4	2
PPT ($mm \cdot day^{-1}$)	23	0	0.5, 3.0
Hm ($g \cdot kg^{-1}$)	16	1	1.5
Bio ($t \cdot ha^{-1}$)	220	20	20
AWC (m)	0.25	0.05	0.05

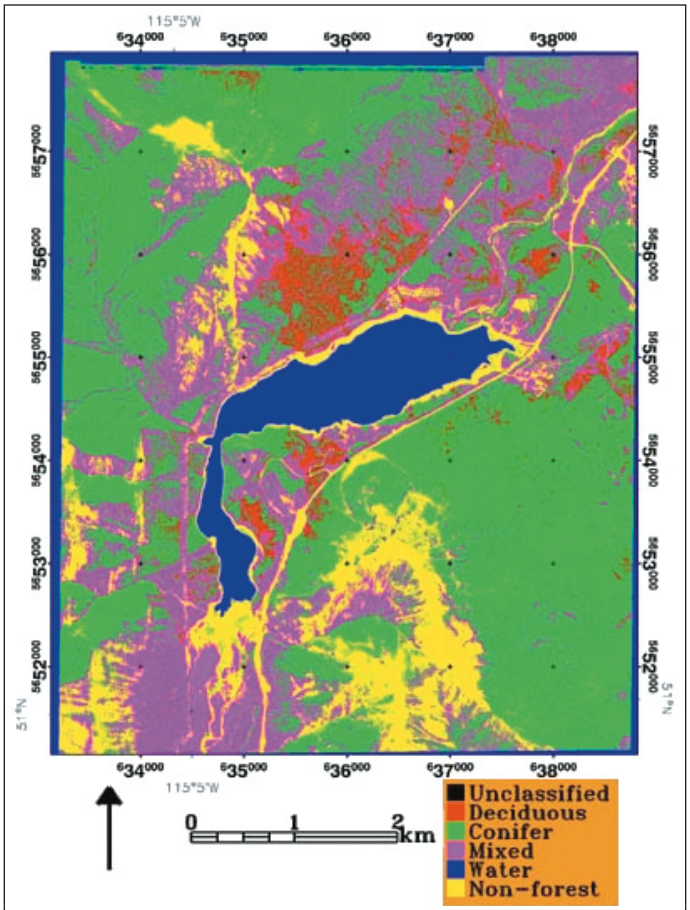

Figure 1. Land cover classification of imagery after the SCS+C topographic correction was applied.

(1) Allometric biomass equations and field-plot data — Unlike LAI, which was measured in each plot, estimates of biomass had to be derived. Allometric equations (**Table 2**) were obtained for Rocky Mountain forest areas in southwestern Alberta from Singh (1982) and used to derive biomass from DBH and tree height field measurements. Based on the number of stems per plot, aboveground dry biomass per unit area ($t \cdot ha^{-1}$) was calculated for all plots.

(2) Empirical models of biomass and LAI at each plot — This step was to relate LAI and biomass at each field plot with the SMA shadow fraction at the corresponding pixel location. This was done using linear regression to establish the statistical relationship between each dependent (Y) variable (LAI, biomass) and the independent (X) variable (SMA shadow fraction, S).

(3) Biomass and LAI estimates over full study area image — Having established equations linking SMA S with LAI and biomass at each field plot, these were then applied at each pixel of the shadow fraction image of the study area. This produced a pixel-by-pixel map of dry biomass ($t \cdot ha^{-1}$) and LAI.

Soil available water capacity (AWC)

Soil moisture is affected by aspect, slope, and elevation and is an important factor influencing the nature and distribution of plant species. Soil water content has been most commonly described by a compound terrain attribute, the wetness index (ϖ) (Band et al., 1993). The calculation of this index is based on the local slope and upslope contributing area affecting the soil moisture status in the calculation unit as

$$\varpi = \ln \frac{A_s}{\tan \beta}, \qquad A_s = \frac{A_T}{\lambda^2} \tag{1}$$

where β is the slope, λ is the ground sampling distance of the pixel, A_s is the specific catchment area, and A_T is the upslope contributing area. Zheng at el. (1996) used this index to estimate soil AWC, and it was found that the index related well to mapping waterlogged soils. This technique was used to estimate AWC for the study area. The wetness index was derived using GIS software functions that derived catchment area and upslope contributing area together with the previously computed terrain derivatives from the DEM. Estimated ϖ ranged from 0 to 15.3. The relationship between ϖ and ground soil series data was established using a digitized soil map of Kananaskis. Some areas adjacent to the lake in the study area were excluded because of their extreme values. A grid linear regression was conducted to estimate AWC as a function of wetness index (AWC = 5.6 × wetness – 6.1). AWC estimates ranged from 0.0 to 28.6 cm, although this could not be validated throughout the study area due to the lack of ground soil series data. The final AWC product is shown in **Figure 2**.

Climate variables

Using meteorological data from the Kananaskis climate station and topographic information, climate variables were extrapolated for each day of the forest growing season of 1 June – 31 August 2003 for solar radiation (Rad), maximum temperature (T_{max}), minimum temperature (T_{max}), precipitation (PPT), and humidity (Hm).

Solar radiation

The amount of solar radiation received at a location influences plant growth and site productivity. The solar radiation algorithm from Swift (1976) was used to calculate the daily total of potential solar radiation on mountain slopes (R_{cor}) as follows:

$$R_{cor} = R_{slope}/R_{horiz}R \tag{2}$$

where R_{slope} ($W \cdot m^{-2}$) is the potential radiation on a slope, R_{horiz} is the potential radiation on a flat surface, and R is the measured radiation on a flat surface (Kananaskis climate station measurement). This method requires an estimate of solar radiation on horizontal surfaces and a ratio, f (slope to flat), to determine how much radiation falls on identically located sloping surfaces. The only inputs necessary for the calculation

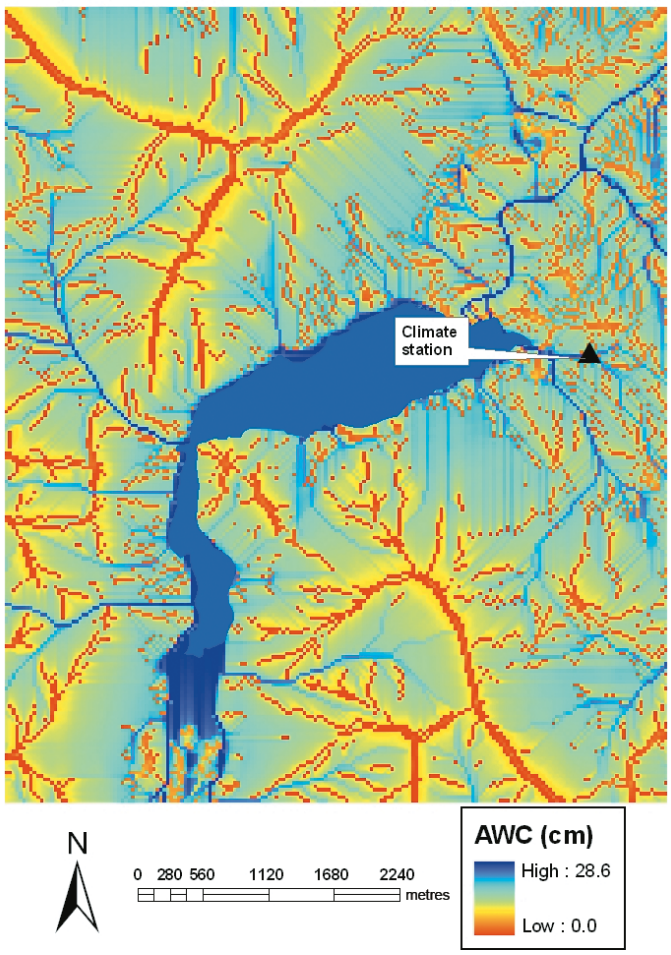

Figure 2. AWC distribution in the study area.

were latitude, slope, aspect, Julian date, and the measured solar radiation at the climate station.

Temperature

Topographic variables, such as altitude, slope, and aspect, play an important role in local surface temperature variations. Lapse rates define the decrease in temperature with increased altitude, and these may vary by aspect. Although the steepness and aspect of a slope affect surface heating and cooling, altitude dominates the topographic influence on temperature variations. Further, no data were available for this area regarding slope or aspect lapse rate adjustments. As a result, the lapse rates used for this study were based on elevation only.

Local lapse rates of –6.0 °C·km^{-1} for maximum temperature and –3.0 °C·km^{-1} for minimum temperature were used based on field data, consistent with established lapse rates elsewhere (Peddle and Duguay, 1995; Bolstada et al., 1998). Daily temperature data were used from the Kananaskis climate station, from which the lapse rates were applied at each pixel according to the elevation difference between the climate station and the pixel elevation from the DEM (Running et al., 1987).

Precipitation

The measured daily precipitation at the Kananaskis climate station was used in conjunction with the ratio of study site monthly precipitation to climate station monthly precipitation (Running et al., 1987; Daly et al., 1994) and with reference to historical precipitation data (30 years). Pixel-based precipitation was then estimated using Equation (3) from Running et al. (1987):

$$P_{cell} = P_{cell0}/P_{b0}P_b \quad (3)$$

where P_{cell} is an estimate of pixel-based precipitation, P_{cell0} is the precipitation throughout the study site from historical isohyet maps, P_{b0} is the precipitation at the climate station from the isohyet maps, and P_b is the precipitation measured at the climate station for the required current year (i.e., 2003).

Humidity

The method for estimating humidity first assumed that daily minimum air temperature was the same as dewpoint ($T_{min} = T_{dew}$) (Running et al., 1987; Thornton et al., 1997). Using the formulations from Murray (1967), saturated vapor pressure (Pa) at the average daytime site temperature T_a (°C) was found using

$$E_s(T_a) = 610.78 \exp\left[\frac{17.269T_a}{273.3 + T_a}\right] \quad (4)$$

where T_a (°C) is the weighted average air temperature of the maximum and minimum air temperatures (T_{max} and T_{min}, respectively) at each pixel (see the Temperature section). T_a was thus estimated per pixel using the following equation from Parton and Logan (1981):

$$T_a = 0.606T_{max} + 0.394T_{min} \quad (5)$$

Ambient vapor pressure (Pa) at the site minimum temperature T_{dew} was then

$$E_m(T_{dew}) = 610.78 \exp\left[\frac{17.269T_{dew}}{273.3 + T_{dew}}\right] \quad (6)$$

from which the relative humidity (Hm) was estimated as

$$Hm = \frac{E_m(T_{dew})}{E_s(T_a)} \times 100 \quad (7)$$

Sensitivity tests of BEPS in Kananaskis forests

Four different types of sensitivity analyses were performed to provide a rigorous test of BEPS. These various tests involve both individual variables and interactions between two or more factors, and thus the overall experimental design provides a comprehensive, rigorous set of tests. **Table 3** shows all of the inputs to BEPS and their value ranges as measured in the study area over the period June to August as a reference for the various test inputs.

NPP sensitivity tests for individual BEPS inputs

A systematic, controlled set of experiments was designed to test the effect of varying each parameter by a constant step throughout a known range, independent of all other parameters (e.g., only a single climate input variable or forest site parameter was altered in a given sensitivity run). Input parameter changes (**Table 4**) were prescribed according to the range and variability measured for the Kananaskis study area (**Table 5**), from which NPP growth from June to August (92 days) was simulated. For a given parameter being tested, the value used for each of the other parameters (being held constant) corresponded to its mean value as measured in the field (**Table 5**).

NPP independent variation tests

To further test the effect of varying each parameter independent of all others, a sensitivity analysis was carried out by varying each parameter from the mean (M) minus one standard deviation (SD), producing NPP (NPP_), to the mean plus one standard deviation, producing NPP (NPP_+), as in White et al. (2000). Among the nine input variables assessed for BEPS, forest type was a nonquantitative, nominal data level factor that does not have associated measures of central tendency (M, SD). Instead, to determine the change of NPP with the variation of forest type, the two most different forest types (conifer and deciduous) were compared. For the other BEPS inputs, a change rate was defined as

$$\text{effect} = (NPP_+ - NPP\_)/NPP_+ \times 100 \quad (8)$$

to assess how each model input varying from $M - SD$ to $M + SD$ affected the modeled NPP output. The larger the rate of change, the more important the individual input in terms of its affect on NPP output (i.e., the sensitivity of the BEPS model to variation of that particular input, with other parameters held constant).

Factorial sensitivity experiment

Fractional factorial analysis is useful for identifying important interactions involving two or more factors (Box et al., 1978). This permitted more complex factor interactions to be assessed compared to the previous two sensitivity analyses that involved individual factors only (see the previous two sections). Of the nine inputs being assessed, all but forest type (nonquantitative) were appropriate for fractional factorial analysis, and thus a one-eighth-fraction factorial analysis was designed (**Table 5**), as in Henderson-Sellers and Henderson-Sellers (1996), from which 32 effects were identified and tested. For n factors in a two-level experiment, 2^n experimental runs were required. For the half-fraction factorial design of full factorials with n parameters, 2^{n-1} simulations were completed, with simulation time halved with results similar to those from the full factorial (Box et al., 1978).

Sensitivity analysis of BEPS to topographic influences

In addition to biophysical and climatic factors, forests are also influenced by topographical variables. For instance, slope, aspect, and elevation can profoundly affect the composition of vegetation. BEPS does not account for this directly, at present. Therefore, the "flat-terrain" approach adapted by the BEPS model could cause biases when applied in mountainous regions (Liu et al., 2003). To test this, the NPP sensitivity analysis was conducted in two steps. BEPS was run using inputs that were not topographically corrected and then run again using inputs that were topographically corrected. Then NPP output with and without topographical correction was compared. Julian day 216 was chosen for the test because it was deemed a typical normal day in terms of daily climate data. For each of the inputs, the model was run twice using the topographically corrected (SCS+C) (Soenen et al., 2005) and uncorrected (original) datasets, with NPP output compared using relative difference:

$$\text{relative difference} = (NPP_{TC} - NPP_o)/NPP_{TC} \times 100 \quad (9)$$

Table 5. Design matrix for eight-factor, one-eighth-fraction factorial experiment.

Run	LAI	Rad	T_{max}	T_{min}	PPT	Hm	Bio	AWC	NPP
1	–	–	–	–	–	+	–	+	1.19
2	+	–	–	–	–	–	+	–	2.00
3	–	+	–	–	–	+	+	–	0.99
4	+	+	–	–	–	–	–	+	2.49
5	–	–	+	–	–	+	–	–	1.18
6	+	–	+	–	–	–	+	+	1.81
7	–	+	+	–	–	+	+	+	0.99
8	+	+	+	–	–	–	–	–	2.39
9	–	–	–	+	–	–	–	–	0.94
10	+	–	–	+	–	+	+	+	1.71
11	–	+	–	+	–	–	+	+	0.66
12	+	+	–	+	–	+	–	–	2.39
13	–	–	+	+	–	–	–	+	0.69
14	+	–	+	+	–	+	+	–	1.07
15	–	+	+	+	–	–	+	–	0.39
16	+	+	+	+	–	+	–	+	2.18
17	–	–	–	–	+	+	+	+	0.89
18	+	–	–	–	+	–	–	–	2.30
19	–	+	–	–	+	+	–	–	1.29
20	+	+	–	–	+	–	+	+	2.19
21	–	–	+	–	+	+	+	–	0.82
22	+	–	+	–	+	–	–	+	2.17
23	–	+	+	–	+	+	–	+	1.36
24	+	+	+	–	+	–	+	–	2.26
25	–	–	–	+	+	–	+	–	0.54
26	+	–	–	+	+	+	–	+	2.11
27	–	+	–	+	+	–	–	+	1.06
28	+	+	–	+	+	+	+	–	1.98
29	–	–	+	+	+	–	+	+	0.19
30	+	–	+	+	+	+	–	–	1.66
31	–	+	+	+	+	–	–	–	0.93
32	+	+	+	+	+	+	+	+	1.68

Note: The plus and minus symbols for the eight parameters set in the simulation indicate the parameter was set at the mean plus 1 SD and the mean minus 1 SD, respectively. The values in the last column show the output 92-day mean NPP (g C m^{-2}·day^{-1}) from each simulation.

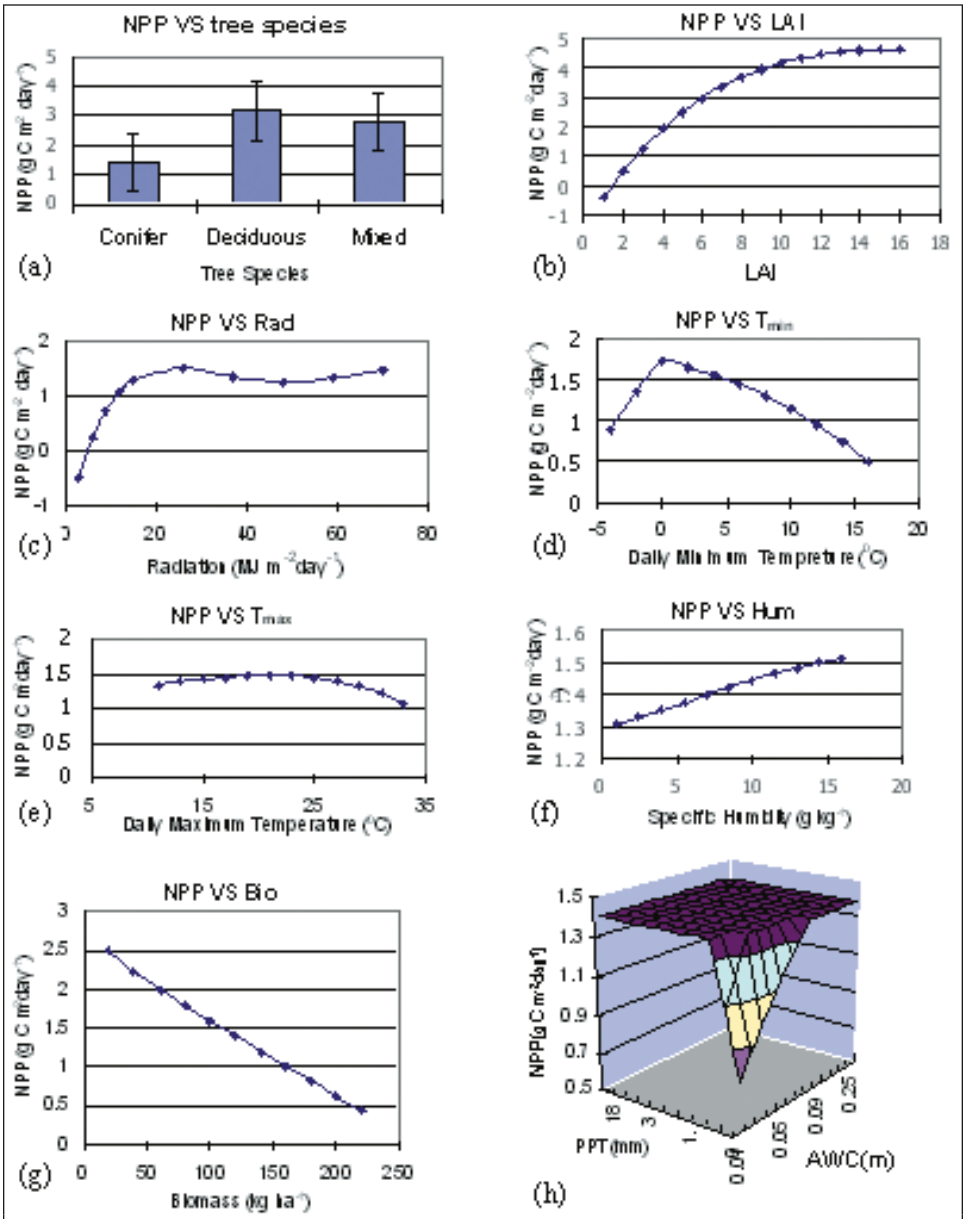

Figure 3. NPP changes with BEPS inputs: (a) forest type; (b) LAI; (c) radiation; (d) minimum temperature (T_{min}); (e) maximum temperature (T_{max}); (f) humidity; (g) biomass; (h) precipitation (PPT) and AWC.

where NPP_{TC} is modeled NPP using the topographically corrected data; and NPP_o is modeled NPP using the original, uncorrected data.

Mapping forest carbon estimates from BEPS

Following the set of comparisons described in the previous sections, the BEPS model was run using all of the topographically corrected inputs to produce NPP estimates for conifer, deciduous, and mixed-wood forests for the mountain growing season (June–August). The distribution of carbon stocks as NPP in the study areas was then mapped from these results.

Results

In this section, the results from the four tests are presented in turn, and each is assessed briefly. An integrated discussion is then presented that synthesizes the large sets of results and identifies major trends in the BEPS carbon model performance.

Results of NPP sensitivity tests for individual BEPS inputs

For this first test, the results from the series of controlled individual experiments (one per test variable) are shown in **Figure 3**. Each test result per variable is presented individually and discussed briefly as follows.

Forest type

For conifer, deciduous, and mixed forests, the average NPP values (**Figure 3a**) from June to August were 1.4, 3.2, and 2.8 g C m^{-2}·day^{-1}, respectively. Deciduous forests had the highest amount of modeled NPP values (per area) compared with the conifer and mixed forest stands. This result is consistent with deciduous stands being generally more productive (for a given set of environmental conditions). This is consistent with the results of Liu et al. (2002) in terms of estimated NPP for different forest types in the Canadian boreal forest.

LAI

According to **Figure 3b**, NPP was very sensitive to LAI. From LAI values of 1–8, NPP had a positive, almost linear relationship with LAI, and the rate of change of NPP was high. The rate of increase of NPP with LAI was less after LAI = 8; beyond LAI = ~12, NPP approached a condition of near saturation (no change in NPP with increased LAI). This indicated that LAI has a considerable impact on NPP estimation because the amount of forest productivity is dependent on the forest canopy to intercept solar energy for photosynthesis.

Solar radiation

Figure 3c shows that NPP was also quite sensitive to the variation of solar radiation, especially when it was less than 25 MJ·m^{-2}·day^{-1}. At higher values of solar radiation, which occurred primarily in mid-June to mid-July, there was little NPP variation. The increase of solar radiation may create water stress, which could accelerate evapotranspiration and thus reduce soil moisture. As a result, the photosynthesis rate decreased. Based on the sensitivity analysis of BEPS inputs, Matsushita et al. (2004) also reported that NPP estimates were sensitive to solar radiation among all climate variables.

Temperature

When the minimum temperature reached 0 °C, forests in the growing season produced the largest amount of NPP (**Figure 3d**). With the increase of daily minimum temperature, both GPP and respiration also increased. Humidity is also a factor. Based on Equations (6) and (7), humidity decreased and the vapor pressure deficit (VPD) would increase. Stomata were closed, GPP was reduced, and forests consumed carbon for respiration, so NPP values decreased when the minimum temperature was above 0 °C. According to **Figure 3e**, when the daily maximum temperature reached 21 °C, NPP reached its highest value. At higher maximum daily temperatures, NPP became lower due to water stress. These results showed both the nature of the BEPS model performance in terms of temperature ranges and the bounding conditions that existed in this mountain environment with respect to carbon dynamics and temperature.

Humidity

Although the influence of humidity on NPP modeling was relatively small (0.2 g C m^{-2}·day^{-1}), **Figure 3f** still shows that the modeled values of NPP were higher with increased humidity. In August, when humidity was reduced compared with June and July, the modeled amount of NPP was reduced. Humidity has a direct effect on regulation of plant stomatal opening. Stomata close when VPD exceeds a critical level (Tibbitts, 1979). Stomatal opening was probably weak when there was a high VPD in the dry environment of the study area (Liu et al., 1999).

Biomass

Theoretically, NPP is expected to increase with increasing forest biomass. Usually forest dry biomass can be directly converted to carbon using a carbon conversion coefficient for different species (Lavigne and Ryan, 1997). In this study, modeled NPP decreased with an increase in biomass (**Figure 3g**). This occurred because biomass used in BEPS was a variable involved in the calculation of forest respiration (R), but not gross primary production (GPP). Therefore, the modeled NPP experienced a (linear) decrease as the forest biomass increased, since NPP was the balance of GPP and R.

Precipitation and soil available water capacity

From the individual model results, both precipitation and AWC (set to average AWC = 0.15 m) had little influence on the estimation of NPP using average precipitation and AWC data measured in the field. Therefore, another modeling test was performed in which precipitation and AWC were varied simultaneously. **Figure 3h** indicates that when daily precipitation was greater than 1.0 mm or AWC was greater than 0.1 m, NPP was not controlled by precipitation, with NPP output as 1.40 g C m^{-2}·day^{-1}. However, at precipitation values of less than 1.0 mm and AWC less than 0.1 m, NPP varied considerably from 0.60 to 1.35 g C m^{-2}·day^{-1}. This was attributed to the well-defined moisture deficit situation from both perspectives.

Results of NPP independent variation tests

Tables 6 and **7** show the results from the sensitivity analysis in which parameters were varied independently from –1 to +1 SD about the mean for the full study area. In **Table 6** the results are shown in terms of percent change and are ranked by absolute value; in **Table 7** the magnitude of effects for all but (nominal level) forest type are shown. The change rates of NPP were interpreted as indicators to determine how important each input was in controlling simulated NPP. According to the sensitivity analysis results, the most important input variables for BEPS were LAI, followed by forest type, biomass, minimum temperature, radiation, maximum temperature, and humidity. For precipitation and AWC, NPP did not change throughout the range of ±1 SD about the mean, because precipitation was still greater than 1 mm and AWC was greater than 0.1 m (see also **Figure 3h** and the previous discussion).

Table 6. Change in simulated mean NPP caused by increasing the parameter from the mean minus 1 SD to the mean plus 1 SD.

Factor	Change (%)	Order of importance[a]
LAI	57.3	1
Tree species	54.2	2
Bio	–30.2	3
T_{min}	–28.8	4
Rad	15.1	5
T_{max}	–8.9	6
Hm	3.3	7
PPT	0	9 (tie)
AWC	0	9 (tie)

[a]Ranked by absolute value of percent change (see Equation (8)).

Table 7. Main effects of parameter variation.

Rank	Factor	Effect
1	LAI	1.143
2	Bio	–0.385
3	T_{min}	–0.383
4	Rad	0.247
5	T_{max}	–0.184
6	Hm	0.031
7	PPT	0.023
8	AWC	0.012

Note: The effect column indicates the NPP (g C m^{-2}·day^{-1}) variation due to increasing a parameter from the mean minus 1 SD to the mean plus 1 SD. The results are ranked by magnitude (absolute value) of effect.

Results of factorial sensitivity experiment

As shown in **Table 8**, the most significant influence of factor interaction effects on NPP was the interaction between daily maximum and minimum temperature (interaction effect of –0.141). Various combinations of LAI, temperature, and solar radiation made up most of the top-ranking interaction effects. However, compared with the main effects (see previous sections), the interaction effects were generally smaller. Also, the order of important input variables for BEPS was similar to that for the results of NPP independent variation sensitivity analysis (**Tables 6** and **7**).

Results of sensitivity analysis for topographic influences

Figure 4 shows the topographic influence on NPP estimation by each BEPS input and the full set of inputs of BEPS (all variables). Precipitation and AWC were excluded in this test because NPP was not sensitive to the average values that were used, as discussed earlier. For the biophysical factors forest type, LAI, and biomass, errors caused by topography appeared to be relatively small. For instance, the total amount of estimated NPP decreased 0.26% for forest type, decreased

Table 8. Results from the fractional factorial tests of two- and three-factor interaction effects of parameter variation.

Rank	Factor	Interaction effect
1	T_{max} × T_{min}	–0.141
2	LAI × Rad	0.093
3	T_{min} × Bio	–0.082
4	Rad × T_{max}	0.075
5	LAI × T_{max}	–0.058
6	Rad × T_{min}	0.047
7	T_{max} × Bio	–0.033
8	T_{max} × AWC	0.032
9	Rad × Hm	0.031
10	PPT × AWC	–0.029
11	T_{max} × PPT	0.023
12	LAI × AWC	0.021
16 (tie)	LAI × Hm	0.017
16 (tie)	Hm × Bio	–0.017
16 (tie)	Hm × Bio × T_{max}	–0.017
16 (tie)	Rad × T_{max} × Bio	0.017
17	Rad × AWC	–0.016
21 (tie)	LAI × Bio	0.011
21 (tie)	PPT × Hm	–0.011
21 (tie)	PPT × Hm × T_{max}	–0.011
21 (tie)	Rad × T_{max} × PPT	0.011
23 (tie)	T_{max} × T_{min} × PPT	–0.005
23 (tie)	T_{min} × PPT	–0.005

Note: The interaction column shows the expected interaction effect on NPP (g C m^{-2}·day^{-1}) caused by varying the shown parameters from the mean minus 1 SD to the mean plus 1 SD. Results are ranked by magnitude (absolute value) of the interaction effect for results that yielded an effect (≠0).

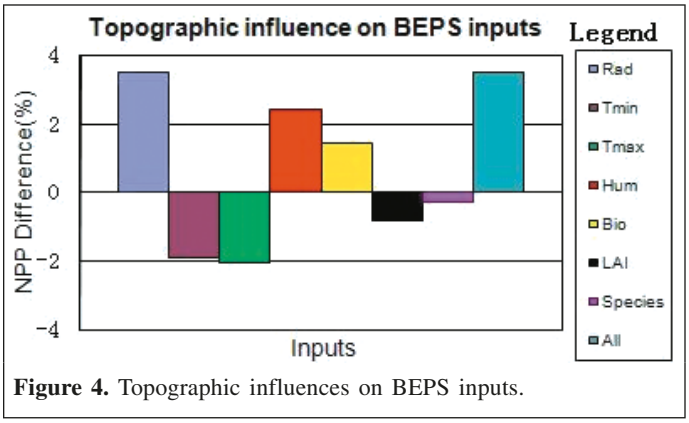

Figure 4. Topographic influences on BEPS inputs.

0.80% for LAI, and increased 1.45% for biomass when using SCS+C topographic correction applied to the satellite imagery compared with that derived from the original, uncorrected data.

The topographic effect on NPP estimation by climate variables was considerably larger than that by forest biophysical factors. When using the SCS+C topographic corrected imagery, modeled NPP increased 3.45% for solar radiation and 2.41% for air humidity and decreased 1.89% for minimum temperature and 2.02% for maximum temperature.

Table 9. Results of NPP estimation for the period June to August.

	Conifer	Deciduous	Mixed	Total
June	46 020.95	5 403.22	37 358.10	88 782.28
July	50 810.06	6 064.57	41 034.38	97 909.01
August	43 312.94	5 687.74	37 677.63	86 678.31
Total (kg C for 92 days)	140 143.96	17 155.54	116 070.11	273 369.60
Avg. (kg C m^{-2})	0.126789	0.145415	0.188510	0.148648
Avg. (kg C m^{-2}·day^{-1})	0.001378	0.001581	0.002049	0.001616

Note: Totals by month and forest type shown together with overall totals, below which are the amount per area and the daily amount for the 92-day period.

In terms of topographic influence on NPP estimation by all the inputs of BEPS, NPP increased by 3.49% using SCS+C topographically corrected inputs compared with original imagery. This is equivalent to an increase of 140 kg C ha^{-1}·$year^{-1}$. As explored in the next section, this represents a significant amount of variation in NPP and carbon estimates. This result indicates that the topographic effect should be accounted for when applying BEPS in mountain environments such as that of our study area.

Forest carbon estimation and mapping

Table 9 shows the BEPS modeled results of NPP for 92 days by month (June to August) for the three forest types. In **Figure 5**, the spatial distribution of NPP was mapped for the study area. The average carbon increase in the study area was ~0.15 kg C m^{-2} during this 3 month period. Carbon accumulation was largest in July, with deciduous forests accounting for a greater portion of that growth compared with other forest types in terms of growth per unit area. Conifers occupy more area (**Figure 5**) overall, but deciduous stands are more productive per unit area than conifers (**Table 9**). Carbon stocks varied throughout the area but were highest in the northeastern quadrant, a primarily northeast-facing front-range slope with more favourable soils and moisture conditions within a mixture of deciduous and mixed forest stands.

Discussion, conclusion, and recommendations

This study implemented a comprehensive methodological framework for sensitivity analysis of net primary productivity (NPP) using satellite imagery. Ground data were acquired in Kananaskis, Alberta, as inputs for the boreal ecosystem productivity simulator (BEPS) model to be parameterized and for validation. A topographic correction performed on satellite imagery was used to assess the influence of topography on NPP modeling. General sensitivity tests were performed for evaluating the effect of each individual BEPS input on NPP estimates and a test of interaction effects involving multiple variables. The topographic sensitivity analysis was performed in the context of assessing BEPS in mountainous terrain, even though the model assumes flat boreal forest terrain. Using the topographically corrected model inputs, NPP was obtained using BEPS for this study area, and an estimate of carbon accumulation was derived. Uncertainties involved in parameterization of the model inputs were documented, and the results of the sensitivity analyses provided important information on the relative importance of both individual parameters and multiple factor interactions, including rank orderings, how the inputs interact, and what parameter inputs were most relevant for BEPS outputs as well as considering these in the topographic context.

Based on the results of the general sensitivity analysis, NPP was sensitive to the variability of field-measured model input data. Leaf area index (LAI) was the most important variable to drive BEPS for NPP modeling according to the results of NPP independent variation sensitivity analysis and the factorial sensitivity tests. This suggests that accurate LAI estimation is essential for proper NPP modeling using BEPS. This individual focus is also supported by the fact that interaction effects of the model inputs were less important compared to individual main effects.

The topographic correction resulted in a 3.5% increase in NPP, corresponding to 140 kg C ha^{-1}·$year^{-1}$. Therefore, to simulate yearly or multiple-year carbon growth in this mountainous region, topographic effects should be taken into account. The climate input variables were more strongly influenced by topography than the forest biophysical inputs (forest type, LAI, biomass). Solar radiation was influenced the most by topography in terms of NPP differences. Solar radiation received by a watershed is the energy source for controlling the growth and activity of plants, and accordingly is one of the prime variables of BEPS. Therefore, accounting for topographic influences on solar radiation loading in complex mountain terrain is deemed necessary. For the Canadian landmass, annual NPP was estimated at 1.22 Gt C $year^{-1}$ in 1994 (Liu et al., 2002). If the topographic influence on NPP estimates is taken into account, there would be an estimated 32.50 Mt C $year^{-1}$ increase for that year.

The average rate of NPP increased during the forest growth season and was estimated using the topographically corrected data (**Table 9**). Annual NPP by the forests in Kananaskis was estimated as 4.01 t C ha^{-1}·$year^{-1}$, obtained as a weighted average from the forest type values of 3.45 t C ha^{-1}·$year^{-1}$ for conifers, 3.95 t C ha^{-1}·$year^{-1}$ for deciduous trees, and 5.12 t C ha^{-1}·$year^{-1}$ for mixed woods from BEPS. This compared well with the field estimate of NPP generated from all available

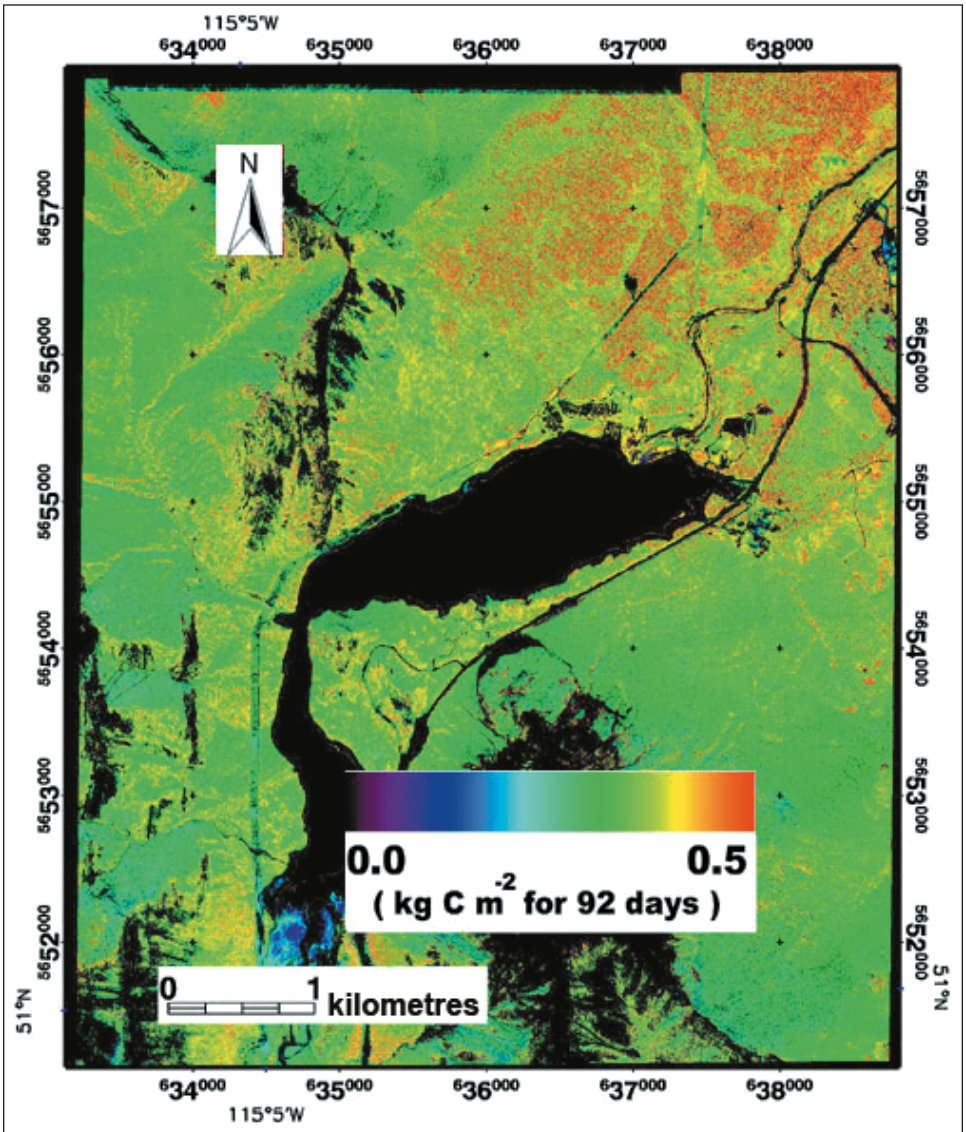

Figure 5. NPP distribution for June to August 2003.

ground plot data of 4.24 t C ha^{-1}·year^{-1}. Deciduous stands were more productive and have larger daily evaporation rates than conifer stands (given the same conditions), as found in the sensitivity results. The highest overall productivity found for mixed forest stands is consistent with the results of Li et al. (2002), who also found mixed-wood NPP was greater than both hardwood and softwood NPP in western Canada using an inventory-based ecosystem model (CBM-CFS2).

Conclusions and recommendations

This research has systematically evaluated the applicability of the ecosystem model BEPS in a complex area of mountainous terrain in Kananaskis, Alberta, Canada. A number of major conclusions and recommendations regarding these sensitivity analyses in the region have been drawn. According to the results of the individual model runs, BEPS NPP was sensitive to most of its inputs. The strongest predictors of NPP for the BEPS model were LAI and forest type, suggesting that these are most important under the range of conditions considered. Also, the interaction effects among input variables were comparatively small versus the main effects from each of the inputs. Particular attention is therefore warranted to maximize the accuracy of these key inputs as individual variables.

The results from the topographic sensitivity showed that topography influenced the NPP estimation in this montane ecosystem. Topography caused negative biases of about 3.5% of the modeled NPP, which is equivalent to 140 kg C ha^{-1}·year^{-1}. Moreover, the climate variables had greater influence than forest biophysical variables, such as LAI, forest type, and biomass. Of all the input variables, solar radiation was influenced the most by topography.

With corrected datasets, the NPP in 2003 was estimated at 4.01 t ha^{-1}·year^{-1}, which was close to the field-measured validation of 4.24 t ha^{-1}·year^{-1}.

This research, for the first time, has assessed the performance of BEPS in a more complex, montane forest setting in the Rocky Mountains that is different from the boreal forest type and flat terrain for which BEPS was designed. The results showed a considerable difference in NPP when topography was addressed using an external correction to input variables. This suggests that the BEPS model, with appropriate inputs and corrections, is a robust model in terms of forest type and terrain, at least for the type of forested terrain involved here.

The influence of topography was shown to be important in this study and was dealt with by topographic correction of the satellite imagery. This is a viable approach, and there are good options to achieve the correction (e.g., Soenen et al., 2005; 2008; Gu and Gillepsie, 1998). Nonetheless, it would be useful to modify the BEPS model directly to handle terrain and not rely on an external correction.

As with any study, there are always ways to improve and refine model inputs, and in this study for BEPS there is latitude for achieving further improvements in carbon estimates, such as more advanced classification, spectral mixture analysis, and canopy reflectance modeling (e.g., Peddle et al., 1999; 2001; 2007). In addition, because carbon cycling is closely related to water dynamics in forest ecosystems, lateral water redistribution (Chen et al., 2007) in mountainous regions could also be taken into account in a future study.

Acknowledgements

This research was supported in part by grants to Dr. Peddle and collaboration from the Natural Sciences and Engineering Research Council of Canada (NSERC), the Alberta Ingenuity Centre for Water Research (AICWR), the Prairie Adaptation Research Collaborative (PARC), the Water Institute for Semiarid Ecosystems (WISE), Natural Resources Canada, and the University of Lethbridge. The Western Canada Research Grid (WestGrid) provided high-performance computing facilities. Scott Soenen, Sam Lieff, and Neal Pilger are thanked for provision of field data, image preprocessing, and other assistance. We are grateful to the staff at the Kananaskis field stations for logistical support in the field, and the Miistakis Institute of the Rockies for provision of the DEM.

References

Amthor, J.S., Chen, J.M., Clein, J.S., Frolking, S.E., Goulden, M.L., Grant, R.F., Kimball, J.S., King, A.W., McGuire, A.D., Nikolov, N.T., Potter, C.S., Wang, S., and Wofsy, S.C. 2001. Boreal forest CO_2 exchange and evapotranspiration predicted by nine ecosystem process models: Intermodel comparisons and relationships to field measurements. *Journal of Geophysical Research*, Vol. 106, pp. 33 623 – 33 648.

Archibald, J.H., Klappstein, G.D., and Corns, I.G.W. 1996. *Field guide to ecosites of southwestern Alberta*. Special Report 8, Canadian Forest Service, Northwest Region, Northern Forestry Centre, Edmonton, Alta. UBC Press, Vancouver, B.C.

Band, L.E. 1993. Effect of land surface representation on forest water and carbon budgets. *Journal of Hydrology*, Vol. 150, pp. 749–772.

Band, L.E., Patterson, P., Nemani, R., and Running, S.W. 1993. Forest ecosystem processes at the watershed scale: incorporating hillslope hydrology. *Agricultural and Forest Meteorology*, Vol. 63, pp. 93–126.

Bolstada, P.V., Swift, L., Collins, F., and Regniere, J. 1998. Measured and predicted air temperatures at basin to regional scales in the southern Appalachian Mountains. *Agricultural and Forest Meteorology*, Vol. 91, pp. 161–176.

Box, G.E.P., Hunter, W.G., and Hunter, J.S. 1978. *Statistics for experimenters*. John Wiley, New York. 653 pp.

Cao, M., and Woodward, F.I. 1998. Dynamic responses of terrestrial ecosystem carbon cycling to global climate change. *Nature (London)*, Vol. 393, pp. 249–252.

Chen, J.M., Liu, J., Cihlar, J., and Goulden, M.L. 1999. Daily canopy photosynthesis model through temporal and spatial scaling for remote sensing applications. *Ecological Modelling*, Vol. 124, pp. 99–119.

Chen, J.M., Chen, W., Liu, J., and Cihlar, J. 2000. Annual carbon balance of Canada's forests during 1895–1996. *Global Biogeochemical Cycles*, Vol. 14, No. 3, pp. 839–850.

Chen, X.F., Chen, J.M., An, S.Q., and Ju, W.M. 2007. Effects of topography on simulated net primary productivity at landscape scale. *Journal of Environmental Management*, Vol. 85, pp. 585–596.

Daly, C., Neilson, R.P., and Phillips, D.L. 1994. A statistical–topographic model for mapping climatological precipitation over mountainous terrain. *Journal of Applied Meteorology*, Vol. 33, pp. 140–158.

Falkowski P., Scholes, R.J., Boyle, E., Canadell, J., Canfield, D., Elser, J., Gruber, N., Hibbard, K., Hogberg, P., Linder, S., Mackenzie, F.T., Moore, B., Pedersen, T., Rosenthal, Y., Seitzinger, S., Smetacek, V., and Steffen, W. 2000. The global carbon cycle: a test of our knowledge of Earth as a system. *Science (Washington, D.C.)*, Vol. 290, No. 13, pp. 291–296.

Friend, A.D., Stevens, A.K., Knox, R.G., and Cannell, M.G.R. 1997. A process-based terrestrial biosphere model of ecosystem dynamics (Hybrid v3.0). *Ecological Modelling*, Vol. 95, pp. 249–287.

Gu, D., and Gillespie, A. 1998. Topographic normalization of LANDSAT TM images of forest based on subpixel sun–canopy–sensor geometry. *Remote Sensing of Environment*, Vol. 64, pp. 166–175.

Hall, F.G., Shimabukuro, Y.E., and Huemmrich, K.F. 1995. Remote sensing of forest biophysical structure using mixture decomposition and geometric reflectance models. *Ecological Applications*, Vol. 5, No. 4, pp. 993–1013.

Hall, R.J., Davidson, D.P., and Peddle, D.R. 2003. Ground and remote estimation of leaf area index in Rocky Mountain forest stands, Kananaskis, Alberta. *Canadian Journal of Remote Sensing*, Vol. 29, No. 3, pp. 411–427.

Hamilton, J.G., DeLucia, E.H., George, K., Naidu, S.L., Finzi, A.C., and Schlesinger, W.H. 2002. Forest carbon balance under elevated CO_2. *Oecologia*, Vol. 131, pp. 250–260.

Henderson-Sellers, B., and Henderson-Sellers, A. 1996. Sensitivity evaluation of environmental models using fractional factorial analysis. *Ecological Modelling*, Vol. 86, pp. 291–295.

Houghton, R.A. 2002. Terrestrial carbon sinks — uncertain explanations. *Biologist*, Vol. 49, No. 4, pp. 155–160.

Houghton, R.A., and Hackler, J.L. 1995. *Continental scale estimates of the biotic carbon flux from land cover change, 1850 to 1980*. Carbon Dioxide

Information Analysis Center, Oak Ridge National Laboratory, Oak Ridge, Tenn. Numeric Data Package NDP-050/R1.

Kurz, W.A., and Apps, M.J. 1999. A 70-year retrospective analysis of carbon fluxes in the Canadian forest sector. *Ecological Applications*, Vol. 9, pp. 526–547.

Lavigne, M.B., and Ryan, G. 1997. Growth and maintenance respiration rates of aspen, black spruce and jack pine stems at northern and southern BOREAS sites. *Tree Physiology*, Vol. 7, pp. 543–551.

Li, Z., Apps, M.J., Banfield, E., and Kurz, W.A. 2002. Estimating net primary production of forests in the Canadian Prairie Provinces using an inventory-based carbon budget model. *Canadian Journal of Forest Research*, Vol. 32, pp. 161–169.

Liu, J., Chen, J.M., Cihlar, J., and Park, W. 1997. A process-based boreal ecosystems productivity simulator using remote sensing inputs. *Remote Sensing of Environment*, Vol. 62, pp. 158–175.

Liu, J., Chen, J.M., Cihlar, J., and Chen, W. 1999. Net primary productivity distribution in the BOREAS region from a process model using satellite and surface data. *Journal of Geophysical Research*, Vol. 104, No. D22, pp. 27 735 – 27 754.

Liu, J., Chen, J.M., Cihlar, J., and Chen, W. 2002. Net primary productivity mapped for Canada at 1-km resolution. *Global Ecology and Biogeography*, Vol. 11, pp. 115–129.

Liu, J., Chen, J.M., and Cihlar, J. 2003. Mapping evapotranspiration based on remote sensing: an application to Canada's landmass. *Water Resources Research*, Vol. 39, No. 7, pp. 1189–1200.

Matsushita, B., Xu, M., Chen, J., Kameyama, S., and Tamura, M. 2004. Estimation of regional net primary productivity (NPP) using a process-based ecosystem model: How important is the accuracy of climate data? *Ecological Modelling*, Vol. 178, pp. 371–388.

Murray, F.W. 1967. On the computation of saturation vapor pressure. *Journal of Applied Meteorology*, Vol. 6, pp. 203–204.

Parton, W.J., and Logan, J.E. 1981. A model for diurnal variation in soil and air temperature. *Agricultural Meteorology*, Vol. 23, pp. 205–216.

Peddle, D.R. 1998. Field spectroradiometer data acquisition and processing for spectral mixture analysis in forestry and agriculture. In *Proceedings of the 1st International Conference on Geospatial Information in Agriculture and Forestry*, 1–3 June 1998, Lake Buena Vista, Fla. ERIM International, Ann Arbor, Mich. Vol. 2, pp. 645–652.

Peddle, D.R., and Duguay, C.R. 1995. Incorporating topographic and climatic GIS data into satellite image analysis of an alpine tundra ecosystem, Front Range, Colorado Rocky Mountains. *Geocarto International*, Vol. 10, No. 4, pp. 43–60.

Peddle, D.R., and Johnson, R.L. 2000. Spectral mixture analysis of airborne remote sensing imagery for improved prediction of leaf area index in mountainous terrain, Kananaskis, Alberta. *Canadian Journal of Remote Sensing*, Vol. 26, No. 3, pp. 177–188.

Peddle, D.R., Hall, F.G., and LeDrew, E.F. 1999. Spectral mixture analysis and geometric–optical reflectance modeling of boreal forest biophysical structure. *Remote Sensing of Environment*, Vol. 67, No. 3, pp. 288–297.

Peddle, D.R., Brunke, S.P., and Hall, F.G. 2001. A comparison of spectral mixture analysis and ten vegetation indices for estimating boreal forest biophysical information from airborne data. *Canadian Journal of Remote Sensing*, Vol. 27, No. 6, pp. 627–635.

Peddle, D.R., Johnson, R.L., Cihlar, J., Leblanc, S.G., Chen, J.M., and Hall, F.G. 2007. Physically based inversion modeling for unsupervised cluster labeling, independent forest classification, and LAI estimation using MFM-5-Scale. *Canadian Journal of Remote Sensing*, Vol. 33, No. 3, pp. 214–225.

Running, S.W. 1994. Testing FOREST-BGC ecosystem process simulations across a climatic gradient in Oregon. *Ecological Applications*, Vol. 4, pp. 238–247.

Running, S.W., and Coughlan, J.C. 1988. A general model of forest ecosystem process for regional applications. 1. Hydrologic balance, canopy gas exchange and primary production processes. *Ecological Modelling*, Vol. 42, pp. 125–154.

Running, S.W., Nemani, R.R., and Hungerford, R.D. 1987. Extrapolation of synoptic meteorological data in mountainous terrain and its use for simulating forest evapotranspiration and photosynthesis. *Canadian Journal of Forest Research*, Vol. 71, No. 6, pp. 472–483.

Singh, T. 1982. *Biomass equations for ten major tree species of the Prairie Provinces*. Northern Forest Centre, Canadian Forest Service, Environmental Canada, Edmonton, Alta. Information Report NOR-X-242.

Soenen, S.A., Peddle, D.R., and Coburn, C. 2005. SCS+C: A modified sun–canopy–sensor topographic correction in forested terrain. *IEEE Transactions on Geoscience and Remote Sensing*, Vol. 43, No. 9, pp. 2149–2160.

Soenen, S.A., Peddle, D.R., Coburn, C.A., Hall, R.J., and Hall, F.G. 2008. Improved topographic correction of forest image data using a 3-D canopy reflectance model in multiple forward mode. *International Journal of Remote Sensing*, Vol. 29, No. 4, pp. 1007–1027.

Swift, L.W. 1976. Algorithm for solar radiation on mountain slopes. *Water Resources Research*, Vol. 12, No. 1, pp. 108–112.

Teillet, P.M., Guindon, B., and Goodenough, D.G. 1982. On the slope-aspect correction of multispectral scanner data. *Canadian Journal of Remote Sensing*, Vol. 8, No. 2, pp. 84–106.

Thornton, P.E., Running, S.W., and White, M.A. 1997. Generating surfaces of daily meteorological variables over large regions of complex terrain. *Journal of Hydrology*, Vol. 190, pp. 214–251.

Tibbitts, T.W. 1979. Humidity and plants. *BioScience*, Vol. 29, No. 6, pp. 358–363.

White, M.A., Thornton, P.E., Running, S.W., and Nemani, R. 2000. Parameterization and sensitivity analysis of the BIOME–BGC ecosystem model: net primary production controls. *Earth Interactions*, Vol. 4, No. 3, pp. 1–85.

Zheng, D.L., Hunt, E.R., Jr., and Running, S.W. 1996. Comparison of available soil water capacity estimated from topography and soil series information. *Landscape Ecology*, Vol. 11, No. 1, pp. 3–14.